CFD Study of Mixing Characteristics in a Torus Reactor

BEKRENTCHIR Khalida [1]; DEBAB Abdelkader [2]; BENMOUSSA Hasnia [3]

1: Laboratoire d'Ingénierie des Procédés de l'Environnement, Université des Sciences et de la Technologie Mohamed Boudiaf,BP 1505 El Mnaouer, Oran, Algeria, *bek.khalida@yahoo.fr*

2: Laboratoire d'Ingénierie des Procédés de l'Environnement, Université des Sciences et de la Technologie Mohamed Boudiaf,BP 1505 El Mnaouer, Oran, Algeria, *Abdelkaderdebab@hotmail.com*

3: Laboratoire d'Ingénierie des Procédés de l'Environnement, Université des Sciences et de la Technologie Mohamed Boudiaf,BP 1505 El Mnaouer, Oran, Algeria, *benmoussahasnia88@yahoo.fr*

Abstract

In this work, the mixing performance in a batch torus reactor was investigated using computational fluid dynamics (CFD). The two impellers applied in this study generated completely different flow patterns: one generates simultaneously axial and rotating motions and the other is particularly shaped for axial pumping.To validate the numerical model, the CFD results for the mean bulk velocity and power number were compared with the experimental data reported in the literature. Next, by solving the numerical dispersion of a passive tracer in an unsteady state, the performance of the torus reactor is investigated in terms of the mixing time. Finally, the numerical tool is used to study the effect of the system geometry and operating conditions on the power consumption and mixing energy. All investigations indicate that the classical three-blade marine impeller has the best mixing performances.

Keywords: *CFD, Torus reactor, Impeller type, Flow pattern, Mixing time, Power consumption*

I. Introduction

In the context of sustainable development, industries are making efforts to improve their processes in order to reduce wastes and therefore contribute to preserve the environment; and among these efforts, the quest for new configurations of reactors more efficient, economic energetically and environment friendly. Because of the disadvantages of the conventional reactors, it became necessary to search other configurations, such as the torus reactor which presents a promising alternative relative to the conventional stirred reactors. Another advantage is the high dispersion achieved because of Dean Vortices involved by the reactor bends, and of the use of a marine screw impeller in the torus axis that generates an efficient three-dimensional swirling motion in the geometry.

The combination of these two effects makes such geometries difficult to experimentally investigate, and thus, to analyse and optimize. In this purpose, computational fluid dynamics (CFD) appears as an interesting tool to investigate the particular hydrodynamic conditions involved in such geometries. However, the modelling of the entire flow in toroidal reactors is not easy, because of the bend curvature effects that have to be accurately represented, and of the impeller that needs to be modelled.

As a preliminary study to flow modelling in torus reactors, J. Pruvost et al. [1] are carried out a numerically study in a well-known standard geometries, namely 90° and 180° bends, with and without swirl motion applied in the bend entry. Different turbulent models and near-wall considerations are considered. The choice of the turbulence model was found to be important. But, despite turbulence is known to be anisotropic in bends [2,3], simple models, based on association of standard wall-functions with k–ε turbulence models, were revealed to be sufficient. In J. Pruvost et al. [4], the numerical investigation is extended to the case of the torus reactor geometry, using a multiple reference frames (MRF) approach to represent the particular flow induced by the impeller.

In this study, CFD was utilized to investigate the effects of different operating conditions and design parameters on the mixing performance of a circular-sectioned torus reactor. To validate the model, the CFD results for the mean bulk velocity and power consumption were compared with the experimental data reported in the literature. The validated CFD model was then used to explore the dependence of mixing time and power consumption on impeller type, impeller diameter and blade angle.

II. Torus reactor description

The reactor in the present simulation is an unbaffled, torus reactor with a circular cross-sectional diameter, D ($=2a$), curvature ratio, $\gamma(=R_C/a)$ and a loop length (L), and the reactor volume is 8 l (Figure 1a). The reactor diameter and curvature ratio are maintained constant in all simulations. The fluid is circulated by rotating an axial flow impeller.

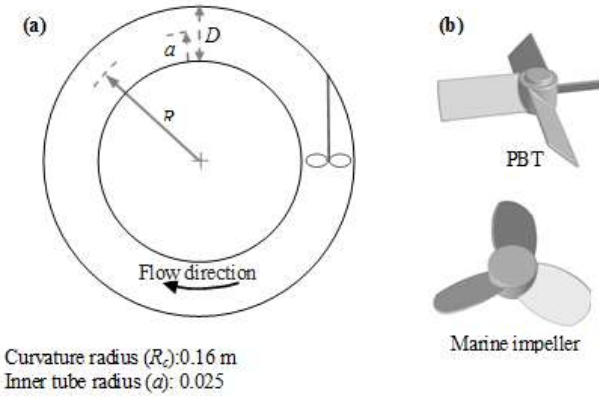

Figure 1 a) Schematic representation of the torus reactor, b) impellers investigated in the present work

Two types of axial flow impeller are used in this study, both of which have diameters of 0.0675 m and a blade pitch angle of 45°. The first impeller is classical (marine impeller) with three pitched flat blades. The second impeller is a four-blade pitched-blade turbine (PBT) (Figure 1b).

III. Grid consideration and boundary conditions

The geometry model of the torus reactor and its mesh are created using GAMBIT, a mesh-generator software package associated with Fluent. Due to the use of MRF resolution, the reactor was divided in non-overlapping regions, a rotating cylindrical volume enclosing the retreat impeller and an outer stationary volume containing the rest of the reactor (Figure 2). The outer stationary volume was also divided in two parts, an irregular part, in the impeller vicinity, and a regular part corresponding to the remaining volume. A regular mesh with elementary hexahedral volumes has been used in the regular part. The grid discretization in this zone is uniform, whereas cells density is gradually increased when coming closer to the impeller. In the irregular part, hybrid meshes are retained, with an irregular zone composed of tetrahedral volumes and prisms.

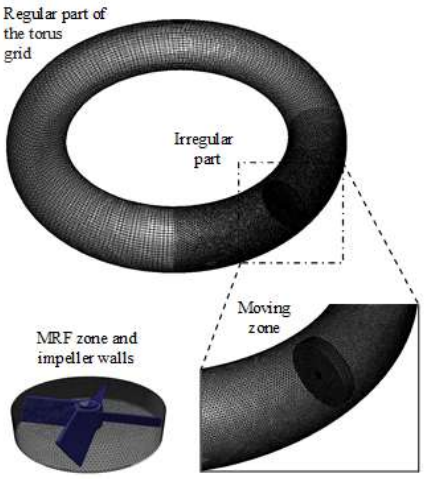

Figure 2 Mesh topology

The torus reactor is of closed type, and the flow result from the impeller rotation is the only driving mechanism. The only boundary condition to be specified in this case was the rotation speed of the impeller. Indeed, with MRF resolution, the impeller is kept stationary, while the rotating frame is given an angular velocity equal to the rotation speed of the impeller. The reactor walls and the impeller surfaces are treated as non-slip boundaries with standard wall functions.

IV. Numerical details

Ak–ω model was used for turbulence modelling. This model was found to give the most accurate prediction by using the commercial code FLUENT in the case of torus shape reactor simulation [1].Based on the mesh created by GAMBIT, Fluent uses a finite volume method to for the discretization of the governing equations over each cell, and then the discrete equations are solved by using a numerical tool along with the boundary conditions. In all simulations, resolution of the algebraic equations was performed using the semi-implicit algorithm pressure linked equation (SIMPLE) with a second-order upwind discretization scheme for

momentum, turbulent kinetic energy and energy dissipation. Solutions are considered to be converged when repeated iterations do not change the power consumption and when the dimensionless velocity residuals remain constant above 10^{-6}. To facilitate the solution convergence, the rotational velocity of the impeller was increased in two or three successive steps, depending of convergence difficulties. Intermediate converged solutions were used to initialize hydrodynamic values for the next higher rotation velocity.

V. Results and discussion

V.1 Validation

To validate the CFD model developed in this study, the CFD results for the mixing Reynolds number were compared with the experimental data reported in the literature.

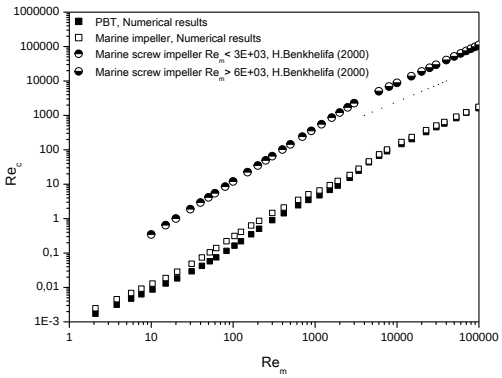

Figure 3 Variation of the circulation Reynolds number with the mixing Reynolds number in continuous and batch conditions.

As depicted in Figure 3, numerical results are in good agreement with the experimental data of H. Benkhelifa et al. [5], confirming the choice of the MRF method for the impeller modeling.

V.2 Investigation of mixing in the torus reactor

To simulate the mixing times after the convergence of the flow field, the unsteady state transport of an inert tracer superimposed on the calculated flow field was monitored until complete homogenization was achieved. The unsteady distribution of the tracer was determined by solving the species transport equation, based on the assumption that the tracer is distributed by convection and diffusion:

$$\frac{\partial C}{\partial t} + U_i \frac{\partial C}{\partial x_i} = \frac{\partial}{\partial x_i}\left[\left(D_j + \frac{\mu_t}{Sc_t}\right)\frac{\partial C}{\partial x_i}\right] \quad (1)$$

where C is the concentration of the passive tracer, Dj is the usual mass diffusion coefficient in the laminar regime, and Ui is the resolved mean velocity component i. The local values of the turbulent viscosity μt are obtained from the turbulence model, and only the turbulent Schmidt number values must be defined to calculate the turbulent mass diffusivity Djt ($Sct = \mu t / \rho Djt$).

The mixing simulation was started by instantaneously adding the tracer at the center of the first bend outlet. Because a passive tracer is used, the mass transport equation does not affect the flow field; thus, only the mass transport equation is solved using the converged-flow-field results. To determine the evolution of the average tracer concentration with respect to time, an unsteady resolution was performed. The second-order implicit scheme was used for time discretization. For each simulated case, different resolutions were performed to verifier that the time step was sufficiently small to not affect the dispersion calculation. The time evolution of the tracer concentration was recorded at the same position as the punctual tracer injection: at the first bend outlet. Before starting the final CFD simulations, several exploratory simulations were performed using the MRF approach to conduct grid independence tests.

The typical evolution of the tracer concentrations for both impellers at two rotation speeds is shown in Figure4: N =900 rpm and N=1000 rpm, which correspond to mixing Reynolds numbers 68000 and 75500, respectively. The tracer averaged concentration on the monitored surface was normalised by the obtained concentration when a total dilution C_{Min} was achieved, which represented the homogeneous tracer concentration. In general, it is observed that all predicted tracer concentration profiles exhibit initial fluctuations, which decay with time and eventually reach a steady-state value. However, the time required for the first concentration peak to appear, its relative height and the time required for the concentration profile to reach the final homogeneous concentration depend on the type of the impeller and the impeller speed.

The obtained values of mixing time for the different conditions are shown as a function of Reynolds number in Figure 5.The mixing time was determined as the time required for the predicted concentration to reach the final homogeneous concentration with a threshold value of 5%.

As depicted in Figure 5, the mixing time rapidly decreases with the increase of the mixing Reynolds number and reaches a constant value for Re_m greater than 30000. However, the mixing times achieved with the marine impeller appear lower than those obtained with the PBT, particularly for low mixing Reynolds numbers. This result is certainly explained by the special design of the marine impeller, which is theoretically better shaped to promote an efficient mixing.

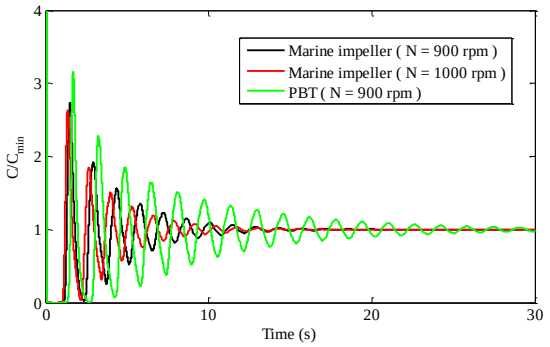

Figure 4 Time evolution of the tracer concentration averaged on the first bend outlet.

Another important parameter to be analysed is the dimensionless mixing time Nt_m [6]. It is noticed that in stirred tanks, this parameter is independent of the mixing Reynolds number for the turbulent regime ($Re_m > 10^4$). In the studied geometry, the evolution of the dimensionless mixing time suggests that a fully turbulent flow regime tends to be achieved at a Reynolds number $Re_m \approx 30000$ (Figure 6). For these two impellers, the marine impeller has lower mixing time values.

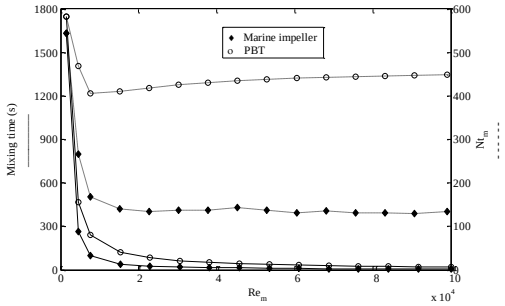

Figure 6 Predicted mixing time as a function of the mixing Reynolds number.

V.3 Power consumption

The power consumption is a crucial characteristic of stirred reactors. This global parameter is particularly useful when comparing the mixing in stirred reactor equipped with different types of impellers.

The power consumption *P*is calculated as the product of the torque, which is derived from the pressure and tangential stress distribution on the moving surfaces (impeller blades and shaft), and the angular velocity [7]:

$$P = 2\pi N \int_A r \times (\tau dA) \qquad (2)$$

where A is the overall impeller and shaft surface area, r is the position vector, and τ is the stress tensor.

For impeller comparison purposes and operation scale-up, the power consumption is often represented in dimensionless form using a power number N_p, which is defined as:

$$N_p = \frac{P}{\rho N^3 d^5} \qquad (3)$$

The predicted values of the power numbers for both impellers are shown as a function of the Reynolds number in Figure 7. These curves show that the power number is inversely proportional to the Reynolds number for low mixing Reynolds numbers and becomes nearly independent of the impeller rotation speed for Re_m greater than 6000. Thus, depending on the Re_m values, the hydrodynamic in the torus reactor can be characterised by three different flow regimes: a laminar regime for mixing Reynolds numbers below 100, a turbulent regime for $Re_m > 6000$, and a transient regime, from laminar behaviour to turbulent behaviour for the mixing Reynolds number range of 10^2-6×10^3, where N_P depends on the Reynolds number. This feature is consistent with the experimental observations of H. Benkhelifa et al. [5]. In particularly, in the turbulent region, $Re_m > 6000$, where N_P tends towards a constant value, the PBT appears to consume less power than the marine impeller: N_P for the marine impeller is 1.23, which is 19.5% higher than that of the PBT. This result is inconsistent with the previous remark that the marine impeller appears to give better mixing.

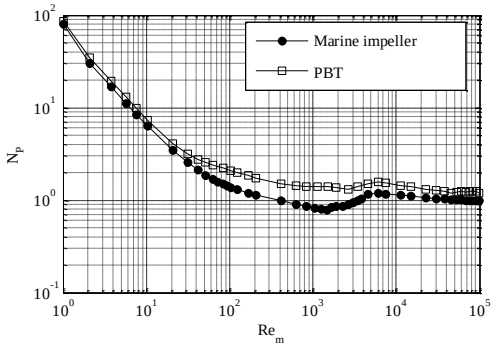

Figure 7 Predicted power number N_P as a function of the mixing Reynolds number

To relate the required time to achieve a specific degree of homogeneity to the power input of the impeller, Nishikawa et al. [8] defined that the product of the mixing time and the power input of the impeller is the mixing energy, which is an index to characterise the mixing in a steered reactor. It should be noted that higher mixing efficiency corresponds to lower mixing energy. As shown in Figure 8, at low impeller speeds, both impellers result in an almost similar mixing energy, whereas for a high Reynolds number, the marine impeller has the best mixing performance, which corresponds to the lowest mixing energy because of the special shape of the blades: curved blades reduce the local energy dissipation rate and lead to better mixing. However, for the PBT, most of the energy is dissipated in the impeller region.

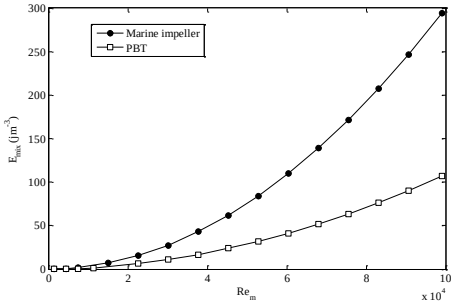

Figure 8 Mixing energy E_{mix}as a function of the mixing Reynolds number.

V. Conclusions

In this study, the mixing performance of the torus reactor was investigated using the Computational fluid dynamics (CFD).To validate the numerical model, the CFD results for the mixing Reynolds number were compared with the experimental data reported in the literature.

Next, by solving numerical dispersion of a passive tracer in unsteady state, performance of the reactor is investigated in term of mixing time. The obtained results show that, regardless of the hydrodynamic condition (rotation speed or impeller type), the achieved mixing time is sufficiently short to rapidly homogenise the concentration in the reactor. Finally, the efficiency of the mixing process was evaluated as the product of the power input and mixing time. For a low impeller rotation speed, both impellers have similar mixing efficiencies, whereas for a high mixing Reynolds number, the classical three-blade marine impeller has the best mixing performances.

Nomenclature

Symbols

a	Inner pipe radius, m
C_j	Passive tracer concentration, mol m^{-3}
C_∞	Homogeneous tracer concentration, mol m^{-3}
d	Impeller diameter, m
D	Pipe diameter, m
E_{mix}	Mixing energy, J m^{-3}
L	Length of the torus reactor, m
N	Rotation velocity of the impeller, rpm
P	Power input by the impeller, W
R_c	Bend curvature radius, m
S_{ct}	Turbulent Schmidt number
t_m	Mixing time, s
U_0	Mean bulk velocity, m s^{-1}

Greek letters

$\gamma(=R_C/a)$	Curvature ratio
μ	Dynamic viscosity, Pa s
ρ	Fluid density, kg m^{-3}

Dimensionless numbers

N_P	Power number
Nt_m	Dimensionless mixing time
$Re_m = \rho N d^2/\mu$	Mixing Reynolds number
$Re_c = \rho U_0 d/\mu$	Circulating Reynolds number

VI. References

[1] J. Pruvost, J. Legrand, P. Legentil homme, Numerical investigation of bend and torus

flows. Part I. Effect of swirl motion on flow structure in U-bend, Chem. Eng. Sci. 59 (16) (2004a) 3345–3357.

[2] K. Sudo, M. Sumida, H. Hibara, Experimental investigation on turbulent flow in a circular-sectioned 90-degrees bend, Exp. Fluids, 25 (1998) 42–49.

[3] M. Anwer, R.M.C. So, Swirling turbulent flow through a curved pipe. Part I: effect of swirl and bend curvature, Exp. Fluids, 14 (1993) 85–96.

[4] J. Pruvost, J. Legrand, P. Legentil homme, J.M. Rosant, Numerical investigation of bend and torus flows. Part II. Flow simulation in torus reactor, Chem. Eng. Sci. 59 (16) (2004) 3359–3370.

[5] H. Benkhelifa, J. Legrand, P. Legentil homme, A. Montillet, Study of the hydrodynamic behaviour of the batch and continuous torus reactors in laminar and turbulent flow regimes by means of tracer methods, Chem. Eng. Sci. 55 (2000) 1871–1882.

[6] M. Bouaifi, M. Roustan, Power consumption, mixing time and homogenization energy in dual-impeller agitated gas–liquid reactors, Chem. Eng. Proc. 40 (2001) 89–95.

[7] A.D. Harvey, C.K. Lee, S.T. Rogers, Steady-state modelling and experimental measurement of a baffled impeller stirred tank, AIChE J. 41 (10) (1995) 2177–2186.

[8] M. Nishikawa, K. Ashiwake, N. Hashimoto, S. Nagata, Agitation power and mixing time in off-centering mixing, Int. Chem. Eng. 19 (1979) 153–159.